AIMS Mathematics, 9(11): 31180–31197.
DOI: 10.3934/math.20241503
Received: 30 August 2024
Revised: 21 October 2024
Accepted: 29 October 2024
Published: 01 November 2024

https://www.aimspress.com/journal/Math

Research article

A new ADI-IIM scheme for solving two-dimensional wave equation with discontinuous coefficients

Ruitao Liu and Wanshan Li*

School of Mathematics and Statistics, Nanjing University of Science and Technology, Nanjing, China.

* **Correspondence:** Email: wsli@njust.edu.cn.

Abstract: A new alternating direction implicit immersed interface method (ADI-IIM) scheme was developed to solve the two-dimensional wave equation with discontinuous coefficients and sources. The alternating direction implicit (ADI) method was equipped with the immersed interface method (IIM) to recover the accuracy as well as maintaining the stability. Numerical experiments were carried out to verify the unconditional stability and the second-order accuracy both in time and space of the proposed scheme.

Keywords: alternating direction implicit method; immersed interface method; discontinuous coefficients; second-order accuracy; unconditional stability
Mathematics Subject Classification: 65M06

1. Introduction

Wave equations are widely used in various engineering and scientific fields, such as the B-ultrasound technology in medicine [1], the oil exploration [2], and the aerospace and biological systems [3]. Meanwhile, material interfaces with discontinuous coefficients on both sides and singular sources are usually encountered in these fields.

There are many numerical methods for solving wave equations without interface, such as finite difference methods [4,5], finite element methods [6], spectral methods [7], and finite volume methods [8]. Specially, as two efficient finite difference schemes for high dimensional problems, the alternating direction implicit (ADI) method and the locally one dimension (LOD) method are both of high accuracy, unconditional stability, and low expense [9–11].

However, when it comes to the case with material interfaces, implementing these numerical schemes to wave equations results in the descent of the accuracy. In order to recover the accuracy, many interface treatments have been proposed, such as immersed boundary method [12, 16], immersed interface method (IIM) [13–17], matched interface and boundary (MIB) method [18], ghost-fluid method [19],

and discontinuous Galerkin method [20]. The IIM is proposed in [21] aiming at solving the elliptic equation with discontinuous coefficients or singular source terms. Based on the jump condition, a correction term is added to the original scheme to retain the spatial accuracy of the scheme. Then, the IIM is extended to parabolic equations and hyperbolic equations with interfaces. The two-grid partially penalized immersed finite element algorithms for solving the semi-linear parabolic interface problems are developed in [14, 15]. Recently, a simple version of the level-set based IIM is developed in [16, 17] to solve the electric potential and its gradient, which avoids the local coordinate transform in the original IIM. For acoustic wave equation in the form of first-order hyperbolic equations in heterogeneous media, a second-order Lax-Wendroff scheme using IIM is developed [22]. For Maxwell's equations with discontinuous material coefficients, an ADI-Yee's scheme through introducing augmented intermediate quantities is proposed, which has advantages such as maintaining the structure as well as the accuracy and stability of Yee's scheme even with the presence of discontinuities [23]. The MIB method recovers the accuracy of the original scheme around the interface by introducing fictitious points to modify the numerical schemes. Values of the fictitious points are determined by approximating the zeroth and first order jump conditions [24]. The advantage of MIB lies in that it avoids the calculation of high order jump conditions. The MIB method is embedded into the finite difference time domain (FDTD) algorithm to propose a new MIBTD scheme to solve the Maxwell's equations with discontinuous coefficients [25].

Furthermore, to improve the stability of the numerical methods for interface problems, many unconditionally stable schemes have been developed. A new algorithm is constructed by combining IIM and LOD methods for the heat conduction equation with interfaces and the unconditional stability is verified numerically [26]. Further, a high-order compact ADI difference scheme with correction terms added by IIM is developed for heat equations with interfaces [27]. The framework of the high-order ADI-FDTD method equipped with the MIB technique is developed to solve Maxwell's equations with straight line interfaces [28]. However, there is little work on the unconditionally stable schemes for 2D wave equation with curve interface.

In this paper, combining IIM and ADI methods, we propose a new scheme for the 2D wave equation with curved interfaces. The influence of the wave speeds in both sides of the interface is considered in the construction of the scheme. For both small jump ratios and large jump ratios, the developed scheme is unconditionally stable and of second order accuracy both in time and space numerically. The rest of this paper is organized as follows. In Section 2, we describe the problems and develop the algorithm. In Section 3, numerical experiments are implemented to verify the unconditional stability and convergence of the proposed scheme. Conclusions are given in Section 4.

2. The description of algorithms

We focus on the initial-boundary value problem of the 2D wave equation with discontinuous coefficients

$$u_{tt} = \alpha\left(u_{xx} + u_{yy}\right) + f(x, y, t), \quad (x, y) \in \Omega, \quad 0 < t \le T, \tag{2.1}$$

$$u(x, y, 0) = \Phi(x, y), \quad u_t(x, y, 0) = \zeta(x, y), \quad (x, y) \in \Omega, \tag{2.2}$$

$$u(x, y, t) = \Psi(x, y, t), \quad (x, y, t) \in \partial\Omega \times (0, T], \tag{2.3}$$

where Ω is a rectangle domain $[a,b]\times[c,d]$ and $\partial\Omega$ is the boundary of Ω. The interface Γ divides Ω into two pieces, denoted by Ω^+ and Ω^-. α is a piecewise constant with values α^+ on Ω^+, and α^- on Ω^-, respectively. Suppose that the following jump conditions are imposed:

$$[u]=\lim_{\substack{x\to\Gamma\\ x\in\Omega^+}}u(x,y,t)-\lim_{\substack{x\to\Gamma\\ x\in\Omega^-}}u(x,y,t)=\omega(x,y,t), \tag{2.4}$$

$$[u_{\boldsymbol{n}}]=\lim_{\substack{x\to\Gamma\\ x\in\Omega^+}}u_{\boldsymbol{n}}(x,y,t)-\lim_{\substack{x\to\Gamma\\ x\in\Omega^-}}u_{\boldsymbol{n}}(x,y,t)=v(x,y,t), \tag{2.5}$$

where $\boldsymbol{n}$ is the outer normal vector; see Figure 1.

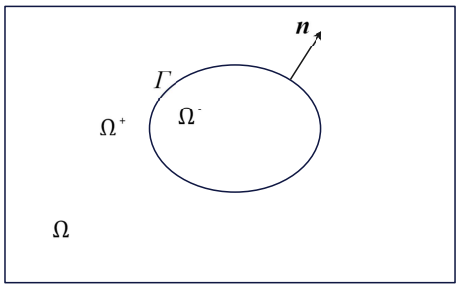

Figure 1. Geometry of the problem.

2.1. Mesh generation

A uniform partition is used with

$$x_i=a+ih_x,\ y_j=c+jh_y,\ t^n=n\tau,\ i=0,1,\cdots,M,\ j=0,1,\cdots,N,\ n=0,1,\cdots,K.$$

where $h_x=(b-a)/M$, $h_y=(d-c)/N$, and $\tau=T/K$.

Let $u_{i,j}^n=u\left(x_i,y_j,t^n\right)$. Define the second-order central difference operators δ_x^2 and δ_y^2

$$\delta_x^2u_{i,j}^n=\frac{u_{i-1,j}^n-2u_{i,j}^n+u_{i+1,j}^n}{h_x^2},\quad \delta_y^2u_{i,j}^n=\frac{u_{i,j-1}^n-2u_{i,j}^n+u_{i,j+1}^n}{h_y^2}.$$

2.2. Construction of the ADI-IIM(2,2) scheme

Following is the construction of the ADI-IIM scheme with second order accuracy both in time and space. For simplicity, we record it as the ADI-IIM(2,2) scheme.

Let $U_{i,j}^n$ be the numerical solution of Eqs (2.1)–(2.5). To start, we give the weighted Crank-Nicolson scheme for Eq (2.1) from t^n to t^{n+1} without interface [29]

$$\begin{aligned}\frac{1}{\tau^2}\left(U_{i,j}^{n+1}-2U_{i,j}^n+U_{i,j}^{n-1}\right)&=\alpha\delta_x^2\left(\theta U_{i,j}^{n+1}+(1-2\theta)U_{i,j}^n+\theta U_{i,j}^{n-1}\right)\\&\quad+\alpha\delta_y^2\left(\theta U_{i,j}^{n+1}+(1-2\theta)U_{i,j}^n+\theta U_{i,j}^{n-1}\right)+f_{i,j}^n,\end{aligned} \tag{2.6}$$

where $0\le\theta\le1$ is the weight.

By introducing the intermediate variable $U^*_{i,j}$, the ADI(2,2) scheme for Eq (2.1) is obtained from Eq (2.6)

$$\textbf{Step 1}: \frac{1}{\tau^2}(U^*_{i,j} - 2U^n_{i,j} + U^{n-1}_{i,j}) = \alpha\delta_x^2\left(\theta U^*_{i,j} + (1-2\theta)\, U^n_{i,j} + \theta U^{n-1}_{i,j}\right) + \alpha\delta_y^2\left((1-2\theta)\, U^n_{i,j} + 2\theta U^{n-1}_{i,j}\right) + f^n_{i,j}, \tag{2.7}$$

$$\textbf{Step 2}: \frac{1}{\tau^2}\left(U^{n+1}_{i,j} - U^*_{i,j}\right) = \alpha\theta\delta_y^2\left(U^{n+1}_{i,j} - U^{n-1}_{i,j}\right). \tag{2.8}$$

Since Eqs (2.7)–(2.8) is a three-level scheme, the values $\left\{U^1_{i,j}\middle|\left(x_i, y_j\right) \in \Omega\right\}$ need to compute first. For $(x_i, y_j) \in \Omega/\partial\Omega$, we use the Taylor series expansion to yield

$$u^1_{i,j} = u^0_{i,j} + \tau u_t\left(x_i, y_j, 0\right) + \frac{\tau^2}{2}u_{tt}\left(x_i, y_j, 0\right) + O\left(\tau^3\right), \tag{2.9}$$

where the term $u_{tt}\left(x_i, y_j, 0\right)$ is replaced by the derivatives in space through the equation (2.1). Then, we develop the numerical scheme for the first time level that

$$U^1_{i,j} = \phi\left(x_i, y_j\right) + \tau\zeta\left(x_i, y_j\right) + \frac{\alpha\tau^2}{2}\left(\phi_{xx} + \phi_{yy}\right)\left(x_i, y_j\right) + \frac{\tau^2}{2}f\left(x_i, y_j, 0\right). \tag{2.10}$$

The scheme (2.7)–(2.8) is unconditional stable when $\theta \in [0.25, 1]$ [29]. In order to solve the problem with interface (2.1)–(2.5), the ADI scheme needs to be modified.

We say $\left(x_i, y_j\right)$ is a regular point if all the five grid points in Eqs (2.7)–(2.8) are on the same side of the interface. At the regular grid point, the local truncation error of the numerical scheme is $O\left(h_x^2 + h_y^2 + \tau^2\right)$.

At the irregular points, suppose that a correction term $F^n_{i,j}$ is added into the right hand side (RHS) of **Step 1**.

$$\frac{1}{\tau^2}\left(U^*_{i,j} - 2U^n_{i,j} + U^{n-1}_{i,j}\right) = \alpha\delta_x^2\left(\theta U^*_{i,j} + (1-2\theta)\, U^n_{i,j} + \theta U^{n-1}_{i,j}\right) + \alpha\delta_y^2\left((1-2\theta)\, U^n_{i,j} + 2\theta U^{n-1}_{i,j}\right) + f^n_{i,j} - F^n_{i,j}, \tag{2.11}$$

where $F^n_{i,j}$ is determined by maintaining the second order accuracy of the scheme. Eqs (2.11) and (2.8) are the proposed ADI-IIM(2,2) scheme of the 2D wave equation with interface (2.1)–(2.5).

The key point lies in the calculation of correction term $F^n_{i,j}$. In the following parts, we provide two algorithms, Algorithm I and Algorithm II, to compute the correction term $F^n_{i,j}$ by applying the methods developed in [16, 26], respectively.

2.3. Calculation of correction term: Algorithm I

In this part, we apply the IIM developed in [26] to the ADI-IIM(2,2) scheme and present Algorithm I for the calculation of correct term $F^n_{i,j}$.

The following lemma is used in the derivation of correction term $F^n_{i,j}$.

Lemma 2.1. *[30] Let $u(x)$ be a piecewise twice differentiable function. Assume that $u(x)$ and its derivatives have finite jumps $[u]$, $[u_x]$, and $[u_{xx}]$, at $x^* = x + \alpha h$, $-1 \le \alpha \le 1$, then the following relations hold,*

$$\frac{u(x+h) - 2u(x) + u(x-h)}{h^2} = u_{xx}(x) + \frac{C_{x2}}{h^2} + O(h), \tag{2.12}$$

where

$$C_{x2} = [u] + [u_x](1 - |\alpha|)h + [u_{xx}]\frac{(1-|\alpha|)^2 h^2}{2}. \tag{2.13}$$

Suppose that $\left(x^*, y_j\right)$ is between $\left(x_i, y_j\right)$ and $\left(x_{i+1}, y_j\right)$, and $\left(x_{i-1}, y_j\right), \left(x_i, y_j\right) \in \Omega^-$, $\left(x_{i+1}, y_j\right) \in \Omega^+$. We have from Lemma 2.1 that

$$\begin{aligned}
\delta_x^2 u_{i,j} =& \frac{u_{i+1,j} - 2u_{i,j} + u_{i-1,j}}{h_x^2} = (u_{xx})_{i,j} + \frac{(C_{x2})_{i,j}}{h_x^2} + O(h_x), \\
\delta_x^2 u_{i+1,j} =& \frac{u_{i+2,j} - 2u_{i+1,j} + u_{i,j}}{h_x^2} = (u_{xx})_{i+1,j} + \frac{(C_{x2})_{i+1,j}}{h_x^2} + O(h_x),
\end{aligned}$$

where

$$\begin{aligned}
(C_{x2})_{i,j} =& [u] + (x_{i+1} - x^*)[u_x] + \frac{(x_{i+1} - x^*)^2}{2}[u_{xx}], \\
(C_{x2})_{i+1,j} =& -[u] - (x_i - x^*)[u_x] - \frac{(x_i - x^*)^2}{2}[u_{xx}].
\end{aligned}$$

Similarly, if $\left(x_{i-1}, y_j\right), \left(x_i, y_j\right) \in \Omega^+$, $\left(x_{i+1}, y_j\right) \in \Omega^-$, it implies that

$$\begin{aligned}
(C_{x2})_{i,j} =& -[u] - (x_{i+1} - x^*)[u_x] - \frac{(x_{i+1} - x^*)^2}{2}[u_{xx}], \\
(C_{x2})_{i+1,j} =& [u] + (x_i - x^*)[u_x] + \frac{(x_i - x^*)^2}{2}[u_{xx}].
\end{aligned}$$

The correction term for the central difference operator in the y direction can be obtained in the same way and we denote it as $(C_{y2})_{i,j}$. Suppose that (x_i, y^*) is between $\left(x_i, y_j\right)$ and $\left(x_i, y_{j+1}\right)$, and $\left(x_i, y_{j-1}\right), \left(x_i, y_j\right) \in \Omega^-$, $\left(x_i, y_{j+1}\right) \in \Omega^+$. We have from Lemma 2.1 that

$$\begin{aligned}
\delta_y^2 u_{i,j} =& \frac{u_{i,j+1} - 2u_{i,j} + u_{i,j-1}}{h_y^2} = \left(u_{yy}\right)_{i,j} + \frac{\left(C_{y2}\right)_{i,j}}{h_y^2} + O\left(h_y\right), \\
\delta_y^2 u_{i,j+1} =& \frac{u_{i,j+2} - 2u_{i,j+1} + u_{i,j}}{h_y^2} = \left(u_{yy}\right)_{i,j+1} + \frac{\left(C_{y2}\right)_{i,j+1}}{h_y^2} + O\left(h_y\right),
\end{aligned}$$

where

$$\left(C_{y2}\right)_{i,j} = [u] + \left(y_{j+1} - y^*\right)\left[u_y\right] + \frac{\left(y_{j+1} - x^*\right)^2}{2}\left[u_{yy}\right],$$

$$\left(C_{y2}\right)_{i,j+1} = -\left[u\right] - \left(y_j - y^*\right)\left[u_y\right] - \frac{\left(y_j - y^*\right)^2}{2}\left[u_{yy}\right].$$

If $\left(y_i, y_{j-1}\right), \left(x_i, y_j\right) \in \Omega^+$, $\left(x_i, y_{j+1}\right) \in \Omega^-$, it implies that

$$\left(C_{y2}\right)_{i,j} = -\left[u\right] - \left(y_{j+1} - y^*\right)\left[u_y\right] - \frac{\left(y_{j+1} - y^*\right)^2}{2}\left[u_{yy}\right],$$

$$\left(C_{y2}\right)_{i,j+1} = \left[u\right] + \left(y_j - y^*\right)\left[u_y\right] + \frac{\left(y_j - y^*\right)^2}{2}\left[u_{yy}\right].$$

To recover the second-order accuracy of the ADI(2,2) scheme for problems with interface, the local truncation errors need to achieve $O\left(h\right)$ at irregular points.

Suppose that (x_i, y_j) is an irregular point. For simplicity, we omit the subscript of space directions in the following contents, assuming that the calculations are all at $\left(x_i, y_j\right)$. The equivalent scheme of the proposed ADI-IIM(2,2) scheme, i.e., Eq (2.11) and Eq (2.8), is written as

$$\frac{U^{n+1} - 2U^n + U^{n-1}}{\tau^2} = M_1^n + M_2^n + M_3^n + f^n - F^n, \tag{2.14}$$

where

$$\begin{aligned}
M_1^n &= \alpha\delta_x^2\left(\theta U^{n+1} + \left(1 - 2\theta\right)U^n + \theta U^{n-1}\right),\\
M_2^n &= \alpha\delta_y^2\left(\theta U^{n+1} + \left(1 - 2\theta\right)U^n + \theta U^{n-1}\right),\\
M_3^n &= -\alpha\tau^2\theta^2\delta_x^2\left[\alpha\delta_y^2\left(U^{n+1} - U^{n-1}\right)\right].
\end{aligned}$$

Replacing the numerical solution U in Eq (2.14) with the exact solution u, we have from the left hand side (LHS) of Eq (2.14) that

$$\frac{u^{n+1} - 2u^n + u^{n-1}}{\tau^2} = u_{tt}^n + O\left(\tau^2\right).$$

For M_1^n on the RHS of Eq (2.14), by Lemma 2.1, it is derived that

$$\begin{aligned}
\widetilde{M}_1^n =& \alpha\theta\delta_x^2 u^{n+1} + \alpha\left(1 - 2\theta\right)\delta_x^2 u^n + \alpha\theta\delta_x^2 u^{n-1}\\
=& \alpha\delta_x^2\left(\theta u^{n+1} + \left(1 - 2\theta\right)u^n + \theta u^{n-1}\right)\\
=& \alpha\delta_x^2\left(u^n + \theta\tau^2 u_{tt}^n + O\left(\tau^4\right)\right)\\
=& \alpha u_{xx}^n + \frac{\alpha C_{x2}^n}{h_x^2} + \alpha\theta\tau^2 u_{ttxx}^n + \frac{\alpha\theta\tau^2 C_{t2x}^n}{h_x^2} + O\left(\frac{\tau^4}{h_x^2} + h_x\right),
\end{aligned} \tag{2.15}$$

where

$$C_{t2x}^n = \begin{cases}
\left[u_{tt}\right], & \left(x_i, y_j\right) \in \Omega^-, \left(x_{i+1}, y_j\right) \in \Omega^+,\\
-\left[u_{tt}\right], & \left(x_i, y_j\right) \in \Omega^+, \left(x_{i+1}.y_j\right) \in \Omega^-,\\
-\left[u_{tt}\right], & \left(x_{i-1}, y_j\right) \in \Omega^-, \left(x_i.y_j\right) \in \Omega^+,\\
\left[u_{tt}\right], & \left(x_{i-1}, y_j\right) \in \Omega^+, \left(x_i, y_j\right) \in \Omega^-.
\end{cases} \tag{2.16}$$

Similarly, for M_2^n, it implies that

$$\widetilde{M}_2^n = \alpha u_{yy}^n + \frac{\alpha C_{y2}^n}{h_y^2} + \alpha\theta\tau^2 u_{ttyy}^n + \frac{\alpha\theta\tau^2 C_{t2y}^n}{h_y^2} + O\left(\frac{\tau^4}{h_y^2} + h_y\right), \tag{2.17}$$

where

$$C_{t2y}^n = \begin{cases} [u_{tt}], & \left(x_i, y_j\right) \in \Omega^-, \left(x_i, y_{j+1}\right) \in \Omega^+, \\ -[u_{tt}], & \left(x_i, y_j\right) \in \Omega^+, \left(x_i.y_{j+1}\right) \in \Omega^-, \\ -[u_{tt}], & \left(x_i, y_{j-1}\right) \in \Omega^-, \left(x_i.y_j\right) \in \Omega^+, \\ [u_{tt}], & \left(x_i, y_{j-1}\right) \in \Omega^+, \left(x_i, y_j\right) \in \Omega^-. \end{cases} \tag{2.18}$$

With respect to M_3^n, we have that

$$\begin{aligned} \widetilde{M}_3^n =& -\alpha\tau^2\theta^2\delta_x^2\left[\alpha\delta_y^2\left(u^{n+1} - u^{n-1}\right)\right] \\ =& -\alpha\tau^2\theta^2\delta_x^2\left[\alpha\delta_y^2\left(2\tau u_t^n + O\left(\tau^3\right)\right)\right] \\ =& -2\alpha\tau^3\theta^2\delta_x^2\left(\alpha\delta_y^2 u_t^n\right) + O\left(\frac{\tau^5}{h_x^2 h_y^2}\right) \\ =& -2\alpha\tau^3\theta^2\delta_x^2\left(\frac{\alpha C_{ty}^n}{h_y^2} + O(1)\right) + O\left(\frac{\tau^5}{h_x^2 h_y^2}\right) \\ =& -\frac{2\alpha\tau^3\theta^2}{h_y^2}\delta_x^2\left(\alpha C_{ty}^n\right) + O\left(\frac{\tau^5}{h_x^2 h_y^2} + \frac{\tau^3}{h_x^2}\right), \end{aligned} \tag{2.19}$$

where

$$C_{ty}^n = \begin{cases} [u_t] + \left(y_{j+1} - y^*\right)\left[u_{ty}\right], & \left(x_i, y_j\right) \in \Omega^-, \left(x_i, y_{j+1}\right) \in \Omega^+, \\ -[u_t] - \left(y_{j+1} - y^*\right)\left[u_{ty}\right], & \left(x_i, y_j\right) \in \Omega^+, \left(x_i.y_{j+1}\right) \in \Omega^-, \\ -[u_t] - \left(y_{j-1} - y^*\right)\left[u_{ty}\right], & \left(x_i, y_{j-1}\right) \in \Omega^-, \left(x_i, y_j\right) \in \Omega^+, \\ [u_t] + \left(y_{j-1} - y^*\right)\left[u_{ty}\right], & \left(x_i, y_{j-1}\right) \in \Omega^+, \left(x_i.y_j\right) \in \Omega^-, \end{cases} \tag{2.20}$$

satisfying $\delta_y^2 u_t^n = C_{ty}^n + O(1)$.

The correction term F^n in Eq (2.14) is given by combining Eqs (2.15)–(2.19),

$$F^n = \frac{\alpha C_{x2}^n}{h_x^2} + \frac{\alpha\theta\tau^2 C_{t2x}^n}{h_x^2} + \frac{\alpha C_{y2}^n}{h_y^2} + \frac{\alpha\theta\tau^2 C_{t2y}^n}{h_y^2} - \frac{2\alpha\tau^3\theta^2}{h_y^2}\delta_x^2\left(\alpha C_{ty}^n\right). \tag{2.21}$$

Calculation of the correction term F^n is based on the jump values of u and its partial derivatives. As these jump conditions are usually defined in the normal direction of the interface, we need to define the local coordinate system at the point (x^*, y^*) on the interface [21]. Define

$$\begin{aligned} \xi &= (x - x^*)\cos\theta + (y - y^*)\sin\theta, \\ \eta &= (x - x^*)\sin\theta + (y - y^*)\cos\theta, \end{aligned}$$

where, the ξ-axis is along the normal direction of the interface, the η-axis is along the tangential direction, and θ is the angle between the x-axis and ξ-axis; see Figure 2.

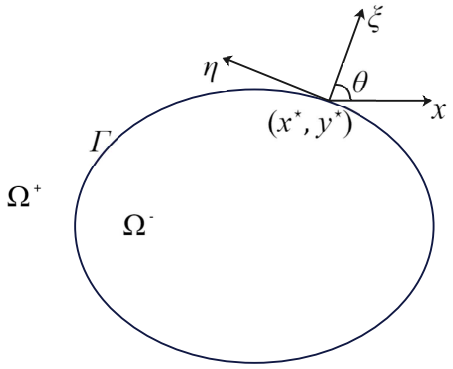

Figure 2. Local coordinate system.

In a neighborhood of the point (x^*, y^*), the interface Γ can be parameterized as

$$\xi = \chi(\eta), \quad \text{with} \quad \chi(0) = 0, \quad \chi'(0) = 0. \tag{2.22}$$

The curvature of the interface at (x^*, y^*) is $\chi''(0)$.

According to jump conditions (2.4)–(2.5), we have the jump conditions in the local coordinate system

$$[u] = \omega(x, y, t) = \widetilde{\omega}(\eta, t), \quad \left[u_\xi\right] = [u_n] = v(x, y, t) = \widetilde{v}(\eta, t). \tag{2.23}$$

Taking the derivative of $[u]$ with respect to η results in

$$\left[u_\eta\right] = \left[u_\xi\right]\chi' + \left[u_\eta\right] = \widetilde{\omega}_\eta(\eta, t). \tag{2.24}$$

Similarly, taking derivatives of $[u_\xi]$ and $[u_\eta]$ with respect to η, it follows by Eq (2.22) that

$$\left[u_{\eta\eta}\right] = -\chi''\left[u_\xi\right] + \widetilde{\omega}_{\eta\eta}, \quad \left[u_{\xi\eta}\right] = \chi''\left[u_\eta\right] + \widetilde{v}_\eta, \tag{2.25}$$

To compute $[u_{\xi\xi}]$, the governing equation (2.1) is written with the same form due to isotropy in local coordinates as

$$u_{tt} = \alpha\left(u_{\xi\xi} + u_{\eta\eta}\right) + f,$$

which replies that

$$\left[u_{\xi\xi}\right] = \left[\frac{u_{tt}}{\alpha}\right] - \left[u_{\eta\eta}\right] - \left[\frac{f}{\alpha}\right]. \tag{2.26}$$

With Eq (2.25), the terms in RHS of Eq (2.26) are easy to compute except $\left[\frac{u_{tt}}{\alpha}\right]$. Now, we focus on the calculation of $\left[\frac{u_{tt}}{\alpha}\right]$.

Considering the influence of the wave speed, i.e., the coefficient α in Eq (2.1), different treatments are taken according to the difference of α^+ and α^-.

Assume that $\alpha^+ > \alpha^-$, and the term in Ω^- is used to represent $\left[\frac{u_{tt}}{\alpha}\right]$, i.e.,

$$\left[\frac{u_{tt}}{\alpha}\right] = \frac{u_{tt}^+}{\alpha^+} - \frac{u_{tt}^-}{\alpha^-} = \frac{u_{tt}^+}{\alpha^+} - \frac{u_{tt}^-}{\alpha^+} + \frac{u_{tt}^-}{\alpha^+} - \frac{u_{tt}^-}{\alpha^-} = \frac{[u_{tt}]}{\alpha^+} + u_{tt}^-\left(\frac{1}{\alpha^+} - \frac{1}{\alpha^-}\right) = \frac{[u_{tt}]}{\alpha^+} + u_{tt}^-\left[\frac{1}{\alpha}\right], \tag{2.27}$$

where u_{tt}^- is obtained by the governing equation and spatial extrapolation. In fact, we have from Eq.(2.1) that

$$u_{tt}^- = \alpha^-\left(u_{xx}^- + u_{yy}^-\right) + f^-. \tag{2.28}$$

The terms u_{xx}^- and u_{yy}^- in RHS of Eq (2.28) are approximated by second-order extrapolation with the nearest grid points around (x^*, y^*) in the domain Ω^-.

When it comes to the case that $\alpha^+ < \alpha^-$, we calculate $\left[\frac{u_{tt}}{\alpha}\right]$ from the other direction, i.e.,

$$\left[\frac{u_{tt}}{\alpha}\right] = u_{tt}^+\left(\frac{1}{\alpha^+} - \frac{1}{\alpha^-}\right) + \frac{[u_{tt}]}{\alpha^-} = \left(\alpha^+ u_{xx}^+ + \alpha^+ u_{yy}^+ + f^+\right)\left[\frac{1}{\alpha}\right] + \frac{[u_{tt}]}{\alpha^-}. \tag{2.29}$$

Finally, through inverse transformation, the jump conditions in the Cartesian coordinates are given:

$$\begin{aligned} [u_x] &= \left[u_\xi\right]\cos\theta - \left[u_\eta\right]\sin\theta, \quad [u_{xx}] = \left[u_{\xi\xi}\right]\cos^2\theta - 2\left[u_{\xi\eta}\right]\cos\theta\sin\theta + \left[u_{\eta\eta}\right]\sin^2\theta, \\ \left[u_y\right] &= \left[u_\xi\right]\sin\theta + \left[u_\eta\right]\cos\theta, \quad \left[u_{yy}\right] = \left[u_{\xi\xi}\right]\sin^2\theta + 2\left[u_{\xi\eta}\right]\cos\theta\sin\theta + \left[u_{\eta\eta}\right]\cos^2\theta. \end{aligned}$$

2.4. Calculation of correction term: Algorithm II

A simple version of IIM for the elliptic equation in an irregular domain is developed in [16]. Compared with the IIM in Section 2.3, for irregular points, the construction and computation of the correction term in the difference scheme by the simple version of IIM relies on the Taylor expansion at the projection point and the surface Laplacian operator, which is implemented without the use of the local coordinate transform. Here, we apply the simple version of IIM to the calculation of the correction term in the ADI-IIM(2,2) scheme Eq (2.11) and Eq (2.8).

In fact, the equivalent scheme of the ADI-IIM(2,2) scheme is obtained by eliminating $U_{i,j}^\star$ from Eq (2.11) and Eq (2.8),

$$\begin{aligned} \frac{1}{\tau^2}\left(U_{i,j}^{n+1} - 2U_{i,j}^n + U_{i,j}^{n-1}\right) = {} & \alpha\delta_x^2\left(\theta U_{i,j}^{n+1} + (1-2\theta)\,U_{i,j}^n + \theta U_{i,j}^{n-1}\right) \\ & + \alpha\delta_y^2\left(\theta U_{i,j}^{n+1} + (1-2\theta)\,U_{i,j}^n + \theta U_{i,j}^{n-1}\right) \\ & - \alpha\theta\tau^2\delta_x^2\left(\alpha\delta_y^2(U_{i,j}^{n+1} - U_{i,j}^{n-1})\right) + f_{i,j}^n - F_{i,j}^n, \end{aligned} \tag{2.30}$$

where $F_{i,j}^n$ is the correction term for the irregular point. It can be seen from Eq (2.30) that a grid point is regular if the standard nine-point Laplacian at that grid point does not cut through the interface, otherwise it is irregular.

To implement the simple version of IIM, the immersed interface Γ in Figure 1 is represented by $\Gamma = \{\boldsymbol{X}(s) = (X(s), Y(s)),\ 0 \le s < 2\pi\}$, where s is a Lagrangian parameter and $\boldsymbol{X}(0) = \boldsymbol{X}(2\pi)$. Also, the level-set function $\phi(x, y)$ of the interface Γ is adopted ([31]).

Take the case illustrated in Figure 3 as an example. Here, the grid point (x_i, y_j) is irregular and the correction term $F_{i,j}^n$ comes from the three points (x_{i-1}, y_{j-1}), (x_{i-1}, y_j), and (x_{i-1}, y_{j+1}) since they fall

into the different side of the interface compared with (x_i, y_j). To derive the correction term as in [16], the orthogonal projections of (x_{i-1}, y_{j-1}), (x_{i-1}, y_j), and (x_{i-1}, y_{j+1}) on the interface, i.e., $\boldsymbol{X}^\star_{k_1}$, $\boldsymbol{X}^\star_k$, and $\boldsymbol{X}^\star_{k_2}$, are determined first as shown in Figure 3. Then, the truncated Taylor's series expansion along the normal direction at the orthogonal projections are given to result in the corresponding correction term

$$F^n_{i,j} = \frac{\alpha^- C^n_{i-1,j}}{h_x^2} - \frac{2\alpha^-\alpha^+\theta\tau^3}{h_x^2 h_y^2}\left(\overline{C}^n_{i-1,j-1} - 2\overline{C}^n_{i-1,j} + \overline{C}^n_{i-1,j+1}\right), \tag{2.31}$$

where

$$\begin{aligned} C^n_{i-1,j} = \widetilde{S}(\phi(x_{i-1}, y_j))\Bigg(& [u(t^n)] + d_{i-1,j}[u_{\boldsymbol{n}}(t^n)] + \frac{d^2_{i-1,j}}{2}\left(\left[\frac{u_{tt}(t^n)}{\alpha}\right] - \left[\frac{f(t^n)}{\alpha}\right] - \kappa[u_{\boldsymbol{n}}(t^n)]\right. \\ & \left. - \frac{1}{|\boldsymbol{X}_s|}\frac{\partial}{\partial s}\left(\frac{1}{|\boldsymbol{X}_s|}\frac{\partial[u(t^n)]}{\partial s}\right)\right) + \theta\tau^2[u_{tt}(t^n)]\Bigg)_{\boldsymbol{X}^\star_k}, \end{aligned} \tag{2.32}$$

$$\overline{C}^n_{i-1,j} = \widetilde{S}(\phi(x_{i-1}, y_j))\left([u_t(t^n)] + d_{i-1,j}[u_{\boldsymbol{n}t}(t^n)]\right)_{\boldsymbol{X}^\star_k}, \tag{2.33}$$

$$\overline{C}^n_{i-1,j-1} = \widetilde{S}(\phi(x_{i-1}, y_{j-1}))\left([u_t(t^n)] + d_{i-1,j-1}[u_{\boldsymbol{n}t}(t^n)]\right)_{\boldsymbol{X}^\star_{k_1}}, \tag{2.34}$$

$$\overline{C}^n_{i-1,j+1} = \widetilde{S}(\phi(x_{i-1}, y_{j+1}))\left([u_t(t^n)] + d_{i-1,j+1}[u_{\boldsymbol{n}t}(t^n)]\right)_{\boldsymbol{X}^\star_{k_2}}, \tag{2.35}$$

with $|\boldsymbol{X}_s| = \sqrt{X'^2(s) + Y'^2(s)}$, κ the local curvature of the interface, d the distance from the grid point to its projection on the interface, and $\widetilde{S}$ the modified sign function defined as

$$\widetilde{S}(x) = \begin{cases} 1, & if\ x > 0, \\ -1, & if\ x \le 0. \end{cases} \tag{2.36}$$

The surface Laplacian operator ([32]) and Eq (2.1) are used in the derivation of Eq (2.32).

The terms in Eqs (2.32)–(2.35) can be computed accurately by the jump conditions in the interface (2.4)-(2.5) except the term $\left[\frac{u_{tt}(t^n)}{\alpha}\right]$, which is dealt with the method given in Section 2.3, Eqs (2.27)–(2.29).

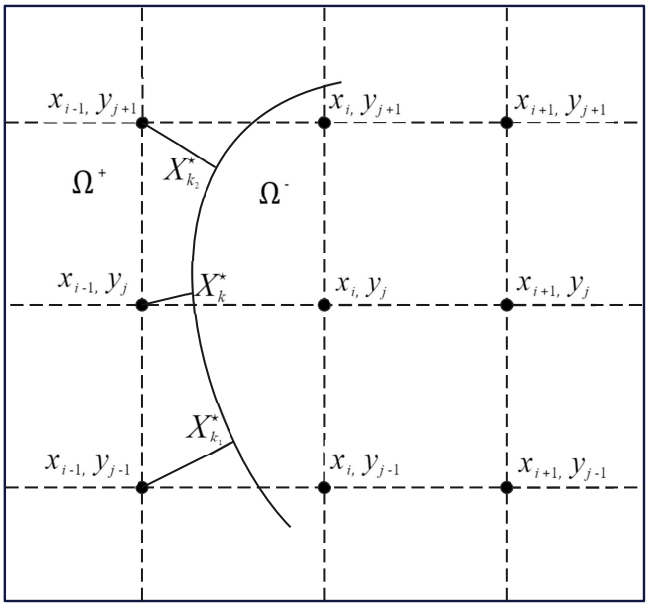

Figure 3. The grid points involved in the equivalent scheme of the ADI-IIM(2,2) scheme at the irregular grid point (x_i, y_j).

3. Numerical experiments

In this section, numerical examples are carried out to verify the unconditional stability and second order convergence of the ADI-IIM(2,2) scheme with Algorithm I and Algorithm II. Define the error function

$$\|\mathrm{Err_u}\|_\infty = \frac{\max\limits_{0\le i\le M,0\le j\le N,0\le n\le K}\left|u^n_{i,j} - U^n_{i,j}\right|}{\max\limits_{0\le i\le M,0\le j\le N,0\le n\le K}\left|u^n_{i,j}\right|}. \tag{3.1}$$

Example 3.1. For Eqs (2.1)–(2.5), suppose that $\Omega = [0,1]\times[0,1]$, $T = 1$, Γ is a circle $(x-0.5)^2 + (y-0.5)^2 = r^2$. Ω^+ represents the domain outside Γ and Ω^- is the domain inside Γ. The coefficient is set as $\alpha = \alpha^+$ in Ω^+ and $\alpha = \alpha^-$ in Ω^-. The exact solution u is taken as

$$u(x,y,t) = \begin{cases} 0, & if\ (x,y) \in \Omega^+, \\ \sin(\pi x)\sin(\pi y)\, e^{\pi t}, & if\ (x,y) \in \Omega^-. \end{cases}$$

The source term is

$$f(x,y,t) = \begin{cases} 0, & if\ (x,y) \in \Omega^+, \\ (1+2\alpha^-)\,\pi^2 \sin(\pi x)\sin(\pi y)\, e^{\pi t}, & if\ (x,y) \in \Omega^-. \end{cases}$$

The jump conditions (2.4)–(2.5) are computed by the exact solution. The proposed ADI-IIM (2,2) scheme with Algorithm I and Algorithm II are used to solve this problem. We take $\theta = 0.4$, $r = 0.21$. Figure 4 displays the shapes of the exact solution, the numerical solutions, and the errors. Figures 4(d)−4(e) show that the errors of the ADI-IIM(2,2) scheme with Algorithm I and Algorithm II are both

within required accuracy, although the errors in domain Ω^- are bigger than those in domain Ω^+ since $u = 0$ for Ω^+. The numerical results are listed in Tables 1–4.

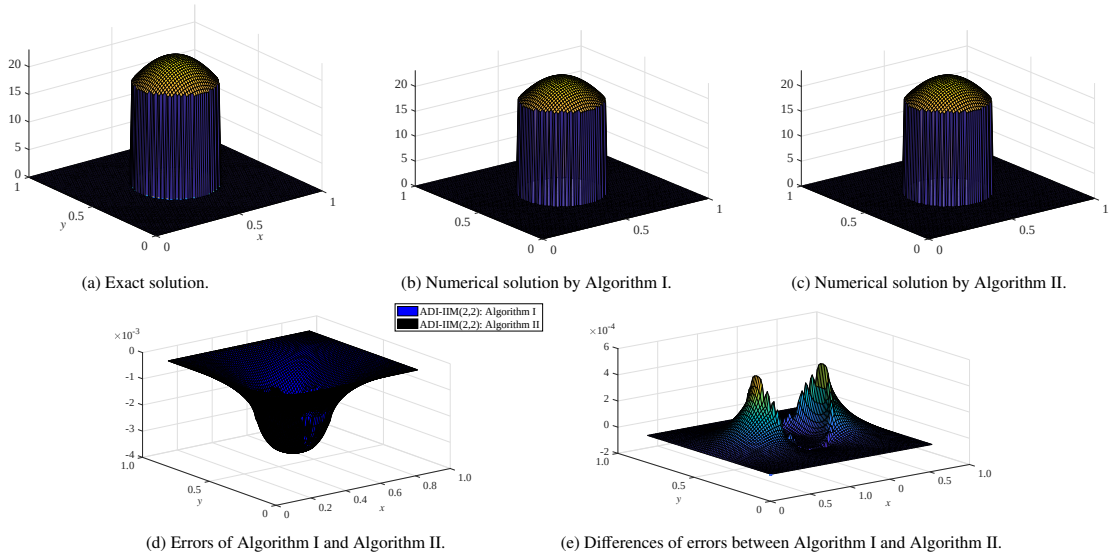

(a) Exact solution. (b) Numerical solution by Algorithm I. (c) Numerical solution by Algorithm II.

(d) Errors of Algorithm I and Algorithm II. (e) Differences of errors between Algorithm I and Algorithm II.

Figure 4. The exact solution, numerical solutions, and errors with $M = N = K = 81$ for Example 3.1.

Table 1. Maximum norm errors of the ADI-IIM(2,2) scheme with small jump ratios ($h_x = 1/M$, $h_y = 1/N$, $\tau = 1/K$, $h_x = h_y = \tau$).

h_x	$\|\mathrm{Err_u}\|_\infty(\alpha^+ = 0.25, \alpha^- = 1)$				$\|\mathrm{Err_u}\|_\infty(\alpha^+ = 1, \alpha^- = 0.25)$			
	Algorithm I	Order	Algorithm II	Order	Algorithm I	Order	Algorithm II	Order
1/21	2.06×10^{-3}	-	2.62×10^{-3}	-	1.87×10^{-3}	-	1.52×10^{-3}	-
1/43	4.30×10^{-4}	2.18	5.45×10^{-4}	2.19	4.71×10^{-4}	1.92	3.67×10^{-4}	1.98
1/81	1.18×10^{-4}	2.05	1.53×10^{-4}	2.00	1.38×10^{-4}	1.94	1.16×10^{-4}	1.83
1/161	2.94×10^{-5}	2.02	3.85×10^{-5}	2.01	3.50×10^{-5}	2.00	2.95×10^{-5}	1.99
1/321	7.17×10^{-6}	2.04	9.62×10^{-6}	2.01	7.99×10^{-6}	2.14	6.69×10^{-6}	2.15

Table 2. Maximum norm errors of the ADI-IIM(2,2) scheme with large jump ratios ($h_x = 1/M$, $h_y = 1/N$, $\tau = 1/K$, $h_x = h_y = \tau$).

h_x	$\|\mathrm{Err_u}\|_\infty(\alpha^+ = 0.01, \alpha^- = 1)$				$\|\mathrm{Err_u}\|_\infty(\alpha^+ = 1, \alpha^- = 0.01)$			
	Algorithm I	Order	Algorithm II	Order	Algorithm I	Order	Algorithm II	Order
1/21	2.07×10^{-3}	-	2.17×10^{-3}	-	2.12×10^{-3}	-	2.12×10^{-3}	-
1/43	4.19×10^{-4}	2.23	4.48×10^{-4}	2.20	5.06×10^{-4}	2.00	5.06×10^{-4}	2.00
1/81	1.11×10^{-4}	2.10	1.21×10^{-4}	2.06	1.43×10^{-4}	2.00	1.43×10^{-4}	2.00
1/161	2.72×10^{-5}	2.05	3.00×10^{-5}	2.03	3.61×10^{-5}	2.00	3.61×10^{-5}	2.00
1/321	6.65×10^{-6}	2.04	7.45×10^{-6}	2.02	9.08×10^{-6}	2.00	9.08×10^{-6}	2.00

For the cases of small jump ratios with $\alpha^+ > \alpha^-$ and $\alpha^- > \alpha^+$, respectively, Table 1 clearly implies the second-order convergence both in time and space of the proposed ADI-IIM(2,2) scheme with Algorithm I and Algorithm II. Also, the robustness of the proposed scheme is verified by the convergence rates shown in Table 2 with the ratio of the discontinuous coefficients is large enough. Moreover, the results of the ADI-IIM(2,2) scheme implemented by Algorithm I and Algorithm II are nearly on the same order of magnitude.

Tables 3 and 4 show the maximum norm errors $\|\mathrm{Err_u}\|_\infty$ of the ADI-IIM(2,2) scheme with large time steps $\tau = lh_x$ ($l = 2, 4, 8, 12$) and long computational time $T = 40$, which demonstrates the unconditional stability of the proposed scheme implemented by Algorithm I or Algorithm II whether the jump ratio is small or large.

Table 3. Maximum norm errors of the ADI-IIM(2,2) scheme for small ratios with large time steps ($T = 40$, $h_x = 1/81$, $h_y = 1/81$, $\tau = lh_x$).

l	$\|\mathrm{Err_u}\|_\infty(\alpha^+ = 0.25, \alpha^- = 1)$		$\|\mathrm{Err_u}\|_\infty(\alpha^+ = 1, \alpha^- = 0.25)$	
	Algorithm I	Algorithm II	Algorithm I	Algorithm II
2	5.94×10^{-4}	8.92×10^{-4}	5.80×10^{-4}	4.186×10^{-4}
4	2.80×10^{-3}	5.33×10^{-3}	2.33×10^{-3}	4.37×10^{-3}
8	1.29×10^{-2}	4.10×10^{-2}	9.42×10^{-3}	3.63×10^{-2}
12	3.28×10^{-2}	1.23×10^{-1}	2.10×10^{-2}	1.12×10^{-1}

Table 4. Maximum norm errors of the ADI-IIM(2,2) scheme for large ratios with large time steps ($T = 40$, $h_x = 1/81$, $h_y = 1/81$, $\tau = lh_x$).

l	$\|\mathrm{Err_u}\|_\infty(\alpha^+ = 0.01, \alpha^- = 1)$		$\|\mathrm{Err_u}\|_\infty(\alpha^+ = 1, \alpha^- = 0.01)$	
	Algorithm I	Algorithm II	Algorithm I	Algorithm II
2	5.71×10^{-4}	6.66×10^{-4}	5.48×10^{-4}	5.47×10^{-4}
4	2.64×10^{-3}	3.42×10^{-3}	2.20×10^{-3}	2.19×10^{-3}
8	1.37×10^{-2}	2.63×10^{-2}	9.33×10^{-3}	1.79×10^{-2}
12	4.40×10^{-2}	8.02×10^{-2}	3.41×10^{-2}	6.03×10^{-2}

Example 3.2. Suppose that $\Omega = [-2, 2] \times [-2, 2]$, $T = 1$, Γ is a circle $x^2 + y^2 = r^2$. Outside of the circle is Ω^+ while inside of the circle is Ω^-. The coefficient $\alpha = \alpha^+$ in Ω^+ and $\alpha = \alpha^-$ in Ω^-. The exact solution u for Eqs (2.1)–(2.5) is

$$u(x, y, t) = \begin{cases} \mathrm{t+sin}\, x \cos y, & if\ (x, y) \in \Omega^+, \\ t + x^2 + y^2, & if\ (x, y) \in \Omega^-. \end{cases}$$

The source term is

$$f(x, y, t) = \begin{cases} (2\alpha^+) \sin x \cos y, & if\ (x, y) \in \Omega^+, \\ -4\alpha^-, & if\ (x, y) \in \Omega^-. \end{cases}$$

We take $\theta = 0.5$ and $r = 0.75$. The numerical results of the ADI-IIM(2,2) scheme with Algorithm I and Algorithm II to solve this problem are displayed in Figure 5 and Tables 5–8. The error plots in

Figure 5(d)–5(e) show that the main errors of the ADI-IIM(2,2) scheme implemented by Algorithm I and Algorithm II arising from the interface are both within required accuracy.

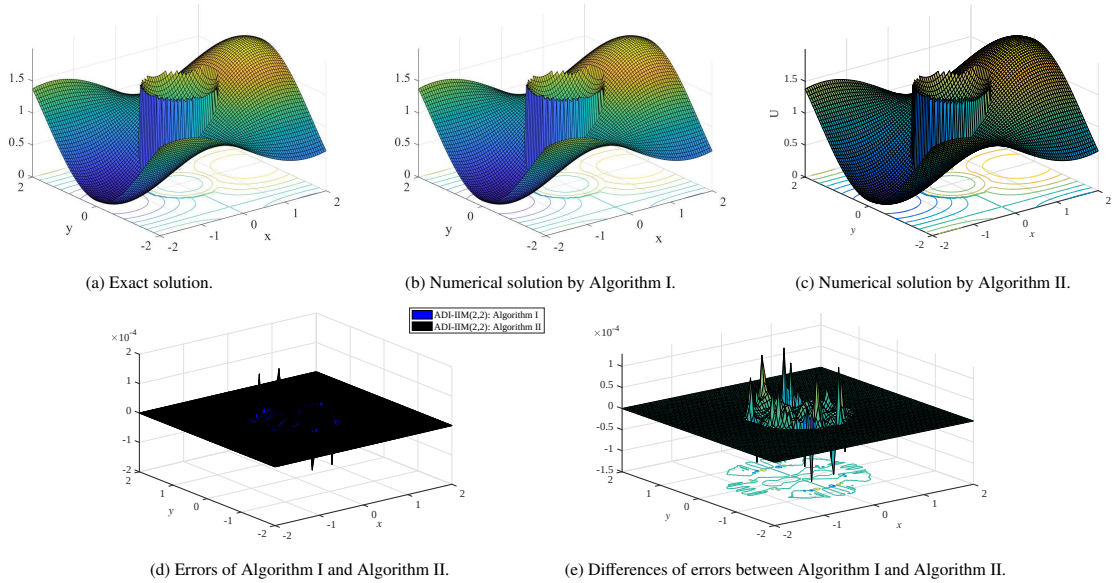

(a) Exact solution. (b) Numerical solution by Algorithm I. (c) Numerical solution by Algorithm II.

(d) Errors of Algorithm I and Algorithm II. (e) Differences of errors between Algorithm I and Algorithm II.

Figure 5. The exact solution, numerical solutions, and errors with $M = N = 81$, $K = 20$ for Example 3.2.

Table 5. Maximum norm errors of the ADI-IIM(2,2) scheme with small jump ratios ($h_x = 4/M$, $h_y = 4/N$, $\tau = 1/K$, $h_x = h_y = \tau$).

h_x	$\|\|\text{Err}_u\|\|_\infty(\alpha^+ = 0.25, \alpha^- = 1)$				$\|\|\text{Err}_u\|\|_\infty(\alpha^+ = 1, \alpha^- = 0.25)$			
	Algorithm I	Order	Algorithm II	Order	Algorithm I	Order	Algorithm II	Order
4/21	1.35×10^{-3}	-	3.75×10^{-4}	-	1.11×10^{-3}	-	7.83×10^{-4}	-
4/41	4.36×10^{-4}	1.69	9.03×10^{-5}	2.28	3.76×10^{-4}	1.61	2.32×10^{-4}	1.94
4/81	8.38×10^{-5}	2.42	2.78×10^{-5}	1.86	8.00×10^{-5}	2.27	6.33×10^{-5}	2.05
4/161	1.54×10^{-5}	2.46	6.44×10^{-6}	2.13	1.97×10^{-5}	2.04	1.60×10^{-5}	2.00
4/321	5.19×10^{-6}	1.58	1.55×10^{-6}	2.07	5.45×10^{-6}	1.86	4.00×10^{-6}	2.01

Table 6. Maximum norm errors of the ADI-IIM(2,2) scheme with large jump ratios ($h_x = 4/M$, $h_y = 4/N$, $\tau = 1/K$, $h_x = h_y = \tau$).

h_x	$\|\|\text{Err}_u\|\|_\infty(\alpha^+ = 0.25, \alpha^- = 1)$				$\|\|\text{Err}_u\|\|_\infty(\alpha^+ = 1, \alpha^- = 0.25)$			
	Algorithm I	Order	Algorithm II	Order	Algorithm I	Order	Algorithm II	Order
4/21	5.38×10^{-4}	-	3.00×10^{-4}	-	1.07×10^{-3}	-	7.86×10^{-4}	-
4/41	2.59×10^{-4}	1.09	5.05×10^{-5}	2.85	3.62×10^{-4}	1.72	2.35×10^{-4}	1.93
4/81	8.39×10^{-5}	1.69	1.73×10^{-5}	1.70	8.55×10^{-5}	2.01	6.55×10^{-5}	2.02
4/161	1.74×10^{-5}	2.25	4.69×10^{-6}	1.90	2.01×10^{-5}	2.11	1.64×10^{-5}	2.01
4/321	4.93×10^{-6}	1.83	8.04×10^{-7}	2.55	5.42×10^{-6}	1.90	4.11×10^{-6}	2.00

Table 7. Maximum norm errors of the ADI-IIM(2,2) scheme for small ratios with large time steps ($T = 40$, $h_x = 4/81$, $h_y = 4/81$, $\tau = lh_x$).

l	$\|\|\text{Err}_\text{u}\|\|_\infty(\alpha^+ = 0.25, \alpha^- = 1)$		$\|\|\text{Err}_\text{u}\|\|_\infty(\alpha^+ = 1, \alpha^- = 0.25)$	
	Algorithm I	Algorithm II	Algorithm I	Algorithm II
2	4.53×10^{-6}	2.03×10^{-6}	1.54×10^{-3}	1.49×10^{-6}
4	5.01×10^{-6}	2.27×10^{-6}	7.58×10^{-3}	1.48×10^{-6}
8	7.00×10^{-6}	4.39×10^{-6}	1.02×10^{-3}	4.86×10^{-6}
12	7.38×10^{-6}	4.69×10^{-6}	1.20×10^{-5}	1.68×10^{-6}

Table 8. Maximum norm errors of the ADI-IIM(2,2) scheme for large ratios with large time steps($T = 40$, $h_x = 4/81$, $h_y = 4/81$, $\tau = lh_x$).

l	$\|\|\text{Err}_\text{u}\|\|_\infty(\alpha^+ = 0.01, \alpha^- = 1)$		$\|\|\text{Err}_\text{u}\|\|_\infty(\alpha^+ = 1, \alpha^- = 0.01)$	
	Algorithm I	Algorithm II	Algorithm I	Algorithm II
2	1.07×10^{-4}	2.07×10^{-6}	2.34×10^{-3}	1.13×10^{-6}
4	1.64×10^{-3}	1.62×10^{-4}	2.69×10^{-1}	5.11×10^{-4}
8	5.90×10^{-6}	8.49×10^{-6}	3.95×10^{-4}	2.36×10^{-5}
12	4.74×10^{-6}	2.41×10^{-6}	9.19×10^{-5}	2.35×10^{-6}

For both of the cases $\alpha^+ > \alpha^-$ and $\alpha^- > \alpha^+$ with either large or small ratios, results in Tables 5 and 6 confirm the second-order convergence both in time and space of the ADI-IIM(2,2) scheme. The maximum norm errors $\|\text{Err}_\text{u}\|_\infty$ in Table 7 and Table 8 show clearly the unconditional stability as well as the robustness of the proposed scheme implemented by Algorithm I and Algorithm II for long computational time $T = 40$ and large time steps.

4. Conclusions

In this paper, we propose a new second-order ADI-IIM numerical scheme with Algorithm I and Algorithm II to solve the 2D wave equation with discontinuous coefficients and sources. The unconditional stability and second order convergence both in time and space are confirmed numerically. In the future, we plan to construct a higher order ADI-IIM scheme with second order in time and fourth-order in space to give more effective simulations of wave propagation in materials with interfaces.

Author contributions

Ruitao Liu: Writing – original draft, Software, Methodology. Wanshan Li: Writing – review & editing, Validation, Supervision, Methodology, Conceptualization, Funding acquisition.

Acknowledgments

Wanshan Li's work was supported by National Natural Science Foundation of China [Grant Numbers 11701282].

Conflict of interest

The authors declare that they have no conflict of interest.

References

1. K. Beklemysheva, G. Grigoriev, N. Kulberg, I. Petrov, A. Vasyukov, Y. Vassilevski, Numerical simulation of aberrated medical ultrasound signals, *Russ. J. Numer. Anal. M.,* **33** (2018), 277–288. http://dx.doi.org/10.1515/rnam-2018-0023
2. R. Alford, K. Kelly, D. Boore, Accuracy of finite-difference modeling of acoustic wave equations, *Geophysics,* **39** (1974), 834–841.
3. A. Taflove, Review of the formulation and applications of the finite-difference time-domain method for numerical modeling of electromagnetic wave interactions with arbitrary structures, *Wave Motion,* **10** (1988), 547–582. http://dx.doi.org/10.1016/0165-2125(88)90012-1
4. D. Deng, C. Zhang, A new fourth-order numerical algorithm for a class of nonlinear wave equations, *Appl. Numer. Math.,* **62** (2012), 1864–1879. http://dx.doi.org/10.1016/j.apnum.2012.07.004
5. W. Wang, H. Zhang, Z. Zhou, X. Yang, A fast compact finite difference scheme for the fourth-order diffusion-wave equation, *Int. J. Comput. Math.,* **101** (2024), 170–193. http://dx.doi.org/10.1080/00207160.2024.2323985
6. D. Shi, L. Pei, Nonconforming quadrilateral finite element method for a class of nonlinear sine-Gordon equations, *Appl. Math. Comput.,* **219** (2013), 9447–9460. http://dx.doi.org/10.1016/j.amc.2013.03.008
7. C. Liu, X. Wu, Arbitrarily high-order time-stepping schemes based on the operator spectrum theory for high-dimensional nonlinear Klein-Gordon equations, *J. Comput. Phys.,* **340** (2017), 243–275. http://dx.doi.org/10.1016/j.jcp.2017.03.038
8. Y. Cui, D. Mao, Numerical method satisfying the first two conservation laws for the Korteweg-de Vries equation, *J. Comput. Phys.,* **227** (2007), 376–399. http://dx.doi.org/10.1016/j.jcp.2007.07.031
9. D. Deng, Q. Wu, The error estimations of a two-level linearized compact ADI method for solving the nonlinear coupled wave equations, *Numer. Algorithms,* **89** (2022), 1663–1693. http://dx.doi.org/10.1007/s11075-021-01168-9
10. X. Yang, W. Qiu, H. Zhang, L. Tang, An efficient alternating direction implicit finite difference scheme for the three-dimensional time-fractional telegraph equation, *Comput. Math. Appl.,* **102** (2021), 233–247. http://dx.doi.org/10.1016/j.camwa.2021-10.021
11. W. Zhang, J. Jiang, A new family of fourth-order locally one-dimensional schemes for the three-dimensional wave equation, *J. Comput. Appl. Math.,* **311** (2017), 130–147. http://dx.doi.org/10.1016/j.cam.2016.07.020
12. C. Peskin, *Lectures on mathematical aspects of physiology. Mathematical aspects of physiology Proceedings of the Twelfth Summer Seminar on Applied Mathematics held at the University of Utah*, Salt Lake City, 1980.

13. J. Gabbard, T. Gillis, P. Chatelain, W. Van Rees, An immersed interface method for the 2D vorticity-velocity Navier-Stokes equations with multiple bodies, *J. Comput. Phys.,* **464** (2022), No. 111339. http://dx.doi.org/10.1016/j.jcp.2022.111339

14. H. Yi, Y. Chen, Y. Wang, Y. Huang, A two-grid immersed finite element method with the Crank-Nicolson time scheme for semilinear parabolic interface problems, *Appl. Numer. Math.,* **189** (2023), 1–22. http://dx.doi.org/10.1016/j.apnum.2023.03.010

15. Y. Wang, Y. Chen, Y. Huang, H. Yi, A family of two-grid partially penalized immersed finite element methods for semi-linear parabolic interface problems, *J. Sci. Comput.,* **88** (2021), 80. http://dx.doi.org/10.1007/s10915-021-01575-z

16. W. Hu, M. Lai, Y. Young, A hybrid immersed boundary and immersed interface method for electrohydrodynamic simulations, *J. Comput. Phys.,* **282** (2015), 47–61. http://dx.doi.org/10.1016/j.jcp.2014.11.005

17. J. Xu, W. Shi, W. Hu, J. Huang, A level-set immersed interface method for simulating electrohydrodynamics, *J. Comput. Phys.,* **400** (2020), 108956. http://dx.doi.org/10.1016/j.jcp.2019.108956

18. D. Nguyen, S. Zhao, Time-domain matched interface and boundary (MIB) modeling of Debye dispersive media with curved interfaces, *J. Comput. Phys.,* **278** (2014), 298–325. http://dx.doi.org/10.1016/j.jcp.2014.08.038

19. C. Li, Z. Wei, G. Long, C. Campbell, S. Ashlyn, S. Zhao, Alternating direction ghost-fluid methods for solving the heat equation with interfaces, *Comput. Math. Appl.,* **80** (2020), 714–732. http://dx.doi.org/10.1016/j.camwa.2020.04.027

20. B. Rivière, S. Shaw, M. Wheeler, J. Whiteman, Discontinuous Galerkin finite element methods for linear elasticity and quasistatic linear viscoelasticity, *Numer. Math.,* **95** (2003), 347–376. http://dx.doi.org/10.1007/s002110200394

21. R. Leveque, Z. Li, The immersed interface method for elliptic equations with discontinuous coefficients and singular sources, *SIAM J. Numer. Anal.,* **31** (1994), 1019–1044. http://dx.doi.org/10.1137/0731054

22. C. Zhang, R. Leveque, The immersed interface method for acoustic wave equations with discontinuous coefficients, *Wave Motion,* **25** (1997), 237–263. http://dx.doi.org/10.1016/S0165-2125(97)00046-2

23. S. Deng, Z. Li, K. Pan, An ADI-Yee's scheme for Maxwell's equations with discontinuous coefficients, *J. Comput. Phys.,* **438** (2021), No. 110356. http://dx.doi.org/10.1016/j.jcp.2021.110356

24. S. Zhao, A matched alternating direction implicit (ADI) method for solving the heat equation with interfaces, *J. Sci. Comput.,* **63** (2015), 118–137. http://dx.doi.org/10.1007/s10915-014-9887-0

25. Y. Zhang, D. Nguyen, K. Du, J. Xu, S. Zhao, Time-domain numerical solutions of Maxwell interface problems with discontinuous electromagnetic waves, *Adv. Appl. Math. Mech.,* **8** (2016), 353–385. http://dx.doi.org/10.4208/aamm.2014.m811

26. J. Liu, Z. Zheng, A dimension by dimension splitting immersed interface method for heat conduction equation with interfaces, *J. Comput. Appl. Math.,* **261** (2014), 221–231. http://dx.doi.org/10.1016/j.cam.2013.10.051

27. J. Liu, Z. Zheng, Efficient high-order immersed interface methods for heat equations with interfaces, *Appl. Math. Mech.,* **35** (2014), 1189–1202. http://dx.doi.org/10.1007/s10483-014-1851-6

28. N. Gong, W. Li, High-order ADI-FDTD schemes for Maxwell's equations with material interfaces in two dimensions, *J. Sci. Comput.,* **93** (2022), 51. http://dx.doi.org/10.1007/s10915-022-02011-6

29. T. Zhang, C. Yu, M. Du, W. Xu, Stability analysis of alternate implicit schemes for 2-D second-order hyperbolic equations, *Second International Conference on Statistics, Applied Mathematics, and Computing Science (CSAMCS 2022), SPIE,* **12597** (2023), 215–221. http://dx.doi.org/10.1117/12.2672453

30. Z. Li, M. Lai, The immersed interface method for the Navier-Stokes equations with singular forces, *J. Comput. Phys.,* **171** (2001), 822–842. http://dx.doi.org/10.1006/jcph.2001.6813

31. S. Osher, R. Fedkiw, Level set methods and dynamic implicit surfaces, *Appl. Math. Sci., Springer,* **153** (2003).

32. J. Xu, H. Zhao, An Eulerian formulation for solving partial differential equations along a moving interface, *J. Sci. Comput.,* **19** (2003), 573–594. http://dx.doi.org/10.1023/A:1025336916176

AIMS Press